Study of inclusive reactions $K^-p \to \bar{K}^0 + X$ and $K^-p \to \Lambda^0 + X$ at 6.5 GeV/c

C. De Clercq, D. P. Johnson, J. Lemonne, P. Peeters, P. Renton,* and J. Wickens
Inter-University Institute for High Energies, ULB-VUB, Brussels, Belgium

B. Musgrave, J. Phelan, P. Schultz, R. Smith, and A. Snyder
Argonne National Laboratory, Argonne, Illinois 60439

R. Ammar, R. Davis, C. Eklund, L. Herder, N. Kwak, L. Loos, R. Riemer, and R. Stump
University of Kansas, Lawrence, Kansas 66045

W. A. Morris, B. Y. Oh, M. Pratap, G. Sionakides, G. A. Smith, and J. Whitmore
Michigan State University, East Lansing, Michigan 48823

F. T. Dao, E. Katsoufis, W. A. Mann, J. Schneps, A. J. Segar, and H. Wald
Tufts University, Medford, Massachusetts 02155

(Received 28 November 1978)

Inclusive V^0 production in 6.5-GeV/c K^-p interactions is studied using the ANL 12-ft-diameter hydrogen bubble chamber. The total cross sections for inclusive $\bar{K}^0$ and Λ^0 production are $\sigma(\bar{K}^0) = 7.98 \pm 0.49$ mb and $\sigma(\Lambda^0) = 3.94 \pm 0.24$ mb. Semi-inclusive differential cross sections are determined as functions of Feynman x and transverse momentum squared of the V^0's, and of four-momentum transfer to the V^0. The average charge multiplicity, the ratio $\langle n_c \rangle / D$, and the correlation function f_2^{cc} for the neutrally charged hadronic system recoiling from the V^0 are determined as functions of the mass of the recoiling system. Results are used to examine universal aspects of multiparticle production.

I. INTRODUCTION

Inclusive $\bar{K}^0$ and Λ^0 production in K^-p interactions has been investigated in a number of bubble-chamber experiments covering the intermediate energy range $3.0 \leq p_{K^-} \leq 16.0$ GeV/c.[1-8] Beam- and target-fragmentation processes are found to dominate inclusive V^0 production, and the relative contributions of simple Regge-exchange processes (Fig. 1) to the kaon- and proton-fragmentation processes have been estimated. For Λ^0 production, the differential cross section and polarization data can be qualitatively described by triple-Regge analyses which invoke the exchange diagrams of Fig. 1(c) and Fig. 1(d). For inclusive $\bar{K}^0$ production, however, analyses of beam-fragmentation processes lead to intercepts $\alpha_{\text{eff}}(0)$ which are inconsistent with dominance of "ρ" exchange [diagram 1(a)]. This is not unexpected since, at 8.2 GeV/c, approximately 40% of the inclusive $\bar{K}^0$ production is associated with K^* production and decay, for which lower-lying trajectories such as the pion trajectory can be exchanged.[5]

In this experiment, measurements are reported concerning semi-inclusive V^0 production at 6.5 GeV/c in reactions

$$K^-p \to \bar{K}^0/K^0 + n_c h^c + \text{anything}, \quad (1)$$

$$K^-p \to \Lambda^0 + n_c h^c + \text{anything}, \quad (2)$$

where $X = (n_c h^c + \text{anything})$ is the neutral hadronic system with charge multiplicity $n_c = 0$, 2, 4, or 6, recoiling from the V^0. Our analysis concentrates on general aspects of V^0 production in K^-p interactions which have not received full attention in previous studies. Differential cross sections are examined as a function of topology; the properties of the charge-multiplicity distributions of the hadronic system recoiling from the V^0 are determined, and are compared with systems having identical additive quantum numbers produced in π^-p, K^+p, $\bar{p}p$, and $\bar{\nu}_\mu p$ processes. The simple qualitative picture which emerges from such comparisons, that charge multiplicities and inclusive distributions from excited hadron systems possess universal features, has been the object of considerable theoretical interest since it may reflect a common, underlying dynamics.[9,10] In the present work, an examination of universal features of

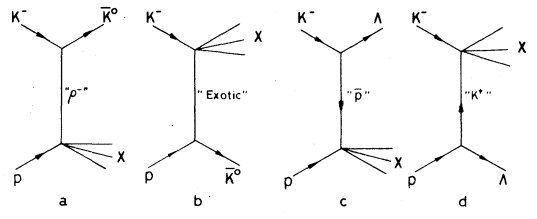

FIG. 1. Regge-exchange diagrams for the inclusive processes $\bar{K}p \to \bar{K}^0 X$ (a), (b) and $\bar{K}p \to \Lambda^0 X$ (c), (d).

multiparticle production at $\sqrt{s} = 3.65$ GeV is presented. Although the center-of-mass energy is relatively low, multiparticle production in 6.5-GeV/c $K^- p$ collisions is found to possess universal features usually ascribed to higher-energy interactions. The deviations from universality which occur in this medium-energy regime are shown to reflect restrictions arising from quantum-number conservation. Results concerning charged multiplicities and features of Λ^0 production in beam- and target-fragmentation regions are discussed in the framework of the quark-interaction model of Brodsky and Gunion.[10]

II. EXPERIMENTAL PROCEDURES

The film was obtained as part of a 75-events/μb exposure in which the ANL 12-ft-diameter hydrogen-filled bubble chamber was exposed to a 6.5-GeV/c K^- beam. An average of about 7 K^- beam particles per picture with less than 5% π^- beam contamination was achieved using a two-stage rf-separated beam line.[11] Separate scans for different event topologies were made independently on unequal portions of film at different laboratories. Events were measured with automatic devices (Polly) or with manual film and image-plane digitizers. The geometrical reconstruction and kinematic fitting were performed using the TVGP-SQUAW or GRIND chain of programs. The V^0's could be classified with little ambiguity as Λ^0 or K_s^0 decays on the basis of three-constraint kinematic fits and by use of the transverse-momentum spectra of the decay products. The distribution of invariant masses of K_S^0 and Λ^0 particles after geometrical reconstruction have FWHM values of 10 and 6 MeV, respectively. Multi-V^0 events were recorded and are included in the analyses of reactions (1) and (2) given below. For inclusive Λ^0 production processes, no correction has been applied to account for Λ^0 particles which are in fact decay products of Σ^0 hyperons. According to the work of Simopolou *et al.* at 8.2 GeV/c,[5] about 10% of Λ^0's originate from Σ^0's.

III. TOPOLOGICAL AND TOTAL INCLUSIVE CROSS SECTIONS

Topological cross sections have been computed using the K^- beam flux determined from the number of τ^- decays recorded in the scans and selected after kinematic fitting. Corrections were applied for scanning, measuring, and kinematic fit inefficiencies, and for losses of V^0's within 1.0 cm and beyond 0.6 meters from the production vertex. The numbers of frames scanned, V^0 events selected, and corresponding cross sections for inclusive $\bar{K}^0$ and Λ^0 production are given in Table I for each topology. All cross sections have been corrected for unseen decay modes.[12]

The total inclusive $\bar{K}^0$ and Λ^0 production cross sections are found to be

$$\sigma(\bar{K}^0) = 7.98 \pm 0.49 \text{ mb},$$

$$\sigma(\Lambda^0) = 3.94 \pm 0.24 \text{ mb}.$$

The contributions from double-V^0 reactions are

$$\sigma(\bar{K}^0 K^0) = 0.31 \pm 0.02 \text{ mb},$$

$$\sigma(\Lambda^0 K^0) = 0.51 \pm 0.03 \text{ mb}.$$

The latter cross section corresponds to reactions of the type

$$K^- p \to \Lambda^0(\Sigma^0) + K\bar{K} + \text{pions} \tag{3}$$

in which hypercharge is not annihilated, in contrast to the reactions

$$K^- p \to \Lambda^0(\Sigma^0) + \text{pions} \tag{4}$$

which contain no particles with hypercharge in the final state.

If it is assumed that all four possible $K\bar{K}$ charge states are produced with comparable cross sections in reactions (3), it follows from the value of $\sigma(\Lambda^0 K^0)$ that inclusive Λ^0 production results predominantly (~85%) from hypercharge-annihilation reactions.

In Figs. 2 and 3, the variation of the topological and total inclusive cross sections for $\bar{K}^0$ and Λ^0 production are shown as a function of incident mo-

TABLE I. Summary of cross sections.

Topology	Number of frames scanned	No. of $\bar{K}^0$ events	$\bar{K}^0$ events/μb	No. of Λ^0 events	Λ^0 events/μb	$\sigma(\bar{K}^0)$ (mb)	$\sigma(\Lambda^0)$ (mb)
Zero-prong V^0	150 000	1 506	1.45	864	2.11	1.04 ± 0.120	0.410 ± 0.050
Two-prong V^0	420 000	11 624	2.54	9287	4.48	4.568 ± 0.401	2.072 ± 0.181
Four-prong V^0	41 200	500	0.22	603	0.47	2.264 ± 0.246	1.298 ± 0.146
Six-prong V^0	22 000	13	0.12	41	0.25	0.107 ± 0.032	0.165 ± 0.036
Total						7.979 ± 0.487	3.945 ± 0.241

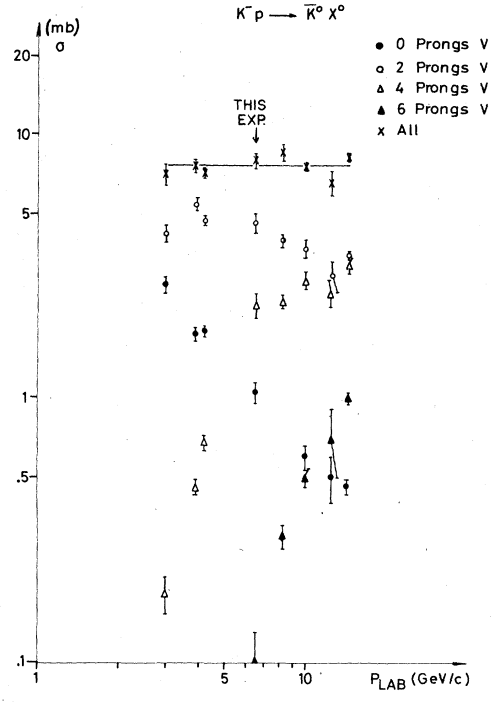

FIG. 2. Topological and inclusive cross sections for $\bar{K}^0$ production in K^-p interactions ($3 < p_{K^-} < 16$ GeV/c). The solid line represents a fit assuming a constant total cross section $\sigma(\bar{K}^0)$.

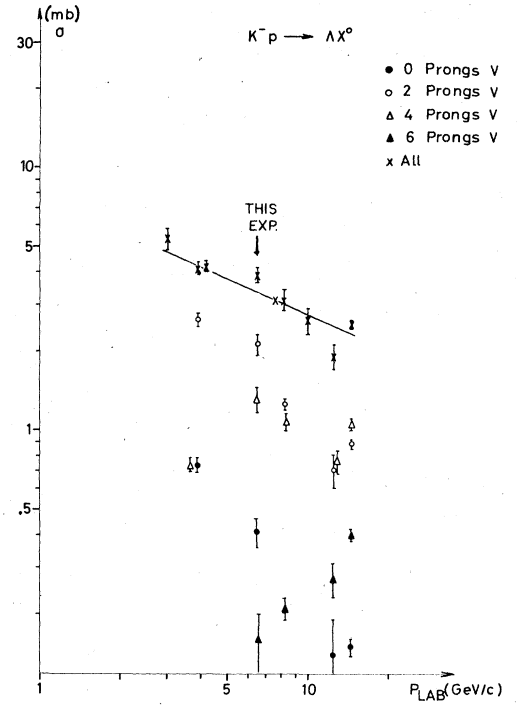

FIG. 3. Topological and total inclusive cross sections for Λ^0 production in K^-p interactions ($3 < p_{K^-} < 16$ GeV/c). The solid line is a fit of the total inclusive $\sigma(\Lambda^0)$ cross section to a power law in the incident K^- momentum (see text).

mentum from 3 to 16 GeV/c. Whereas the total inclusive $\bar{K}^0$ cross section is almost independent of the incident K^- momentum p_{K^-}, the cross section for reaction (2) which is mainly due to hypercharge annihilation, decreases with p_{K^-}. A fit of inclusive Λ^0 production data to the simple power law $\sigma(\Lambda^0) = a p_{K^-}{}^{-b}$ yields $a = 7.61 \pm 0.08$ and $b = 0.444 \pm 0.004$, with χ^2 probability of 0.1%. A fit of the inclusive-cross-section data for $\bar{K}^0$ production to a constant value as shown in Fig. 2 yields $\sigma_{K^-}(\bar{K}^0) = 7.69 \pm 0.11$ mb with χ^2 probability of 5%. An approximately constant K^0-production cross section is also found in K^+p interactions throughout the same incident momentum regime, but with a lower value, $\sigma_{K^+}(K^0) \simeq 5.7$ mb.[7] Since K^-p and K^+p interactions lead to different isospin mixtures, the inclusive cross sections $\sigma_{K^-}(\bar{K}^0)$ and $\sigma_{K^+}(K^0)$ should not be expected to be equal. In particular, "charge-annihilation" states cannot occur in K^+p interactions. At 6.5 GeV/c, the absence of the zero-V topology in K^+p interactions accounts for approximately half of the total inclusive K^0 cross section difference $\sigma_{K^-}(\bar{K}^0) - \sigma_{K^+}(K^0) \simeq 2$ mb.

IV. DIFFERENTIAL CROSS SECTIONS

Figures 4 and 5 show the distributions of the missing mass squared $M_X{}^2$ recoiling from V^0's produced in reactions (1) and (2), respectively. The mass of the system recoiling from $\bar{K}^0$ mesons has a smooth distribution, apart from evidence for charge-exchange neutron production observed in the zero-prong-vee topology. The spectrum for Λ^0 production shows definite structure in the zero- and two-prong V^0 topologies. Evidence for $\Lambda\pi^0$ and $\Lambda\phi^0$ quasi-two-body processes is clearly seen in the zero-prong V^0 final states, whereas ρ, ω, and possibly η' production is observed in the two-prong V^0 distribution. For sufficiently high invariant-mass values ($M_X{}^2 > 2$ GeV^2), the mass distribution integrated over all topologies has an exponential shape, which can be understood from phase-space considerations as shown by Beaupre *et al.*[6] The results of fits of the invariant-mass distributions to the expression $d\sigma/dM_X = \sigma_0 e^{kM_X}$ are

$$\sigma_0(\bar{K}) = 19.9 \pm 2.28 \ \mu\text{b/GeV}$$

and

$$k_K = 2.18 \pm 0.05 \ \text{GeV}^{-1}$$

for $1.5 < M_X < 3.0$ GeV (χ^2 probability = 74%),

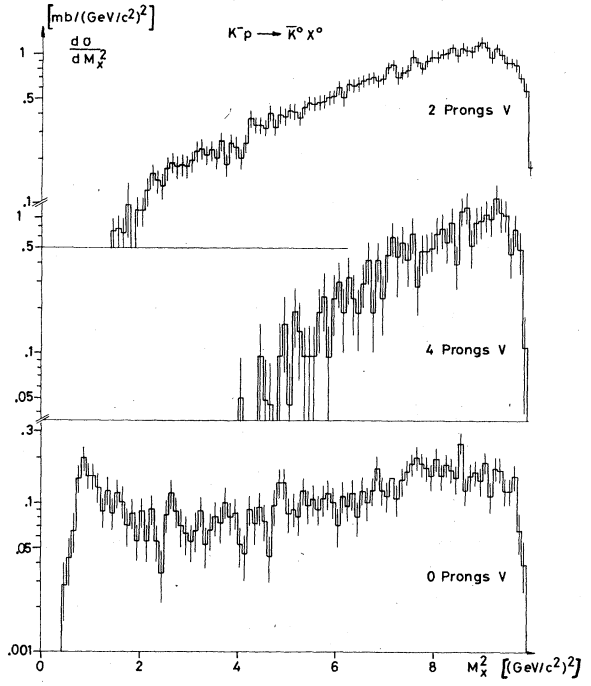

FIG. 4. Distribution of the missing mass squared M_X^2 recoiling from the $\overline{K}^0$ emitted in the reaction $K^-p \to \overline{K}^0 X$. Events are subdivided by topology.

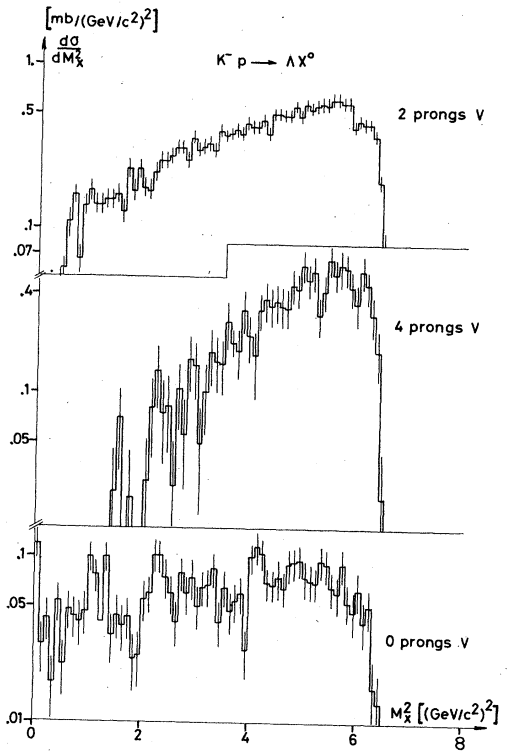

FIG. 5. Distribution of the missing mass squared M_X^2 recoiling from the Λ^0 emitted in the reaction $K^-p \to \Lambda^0 X$. Events are subdivided by topology.

$$\sigma_0(\Lambda) = 53.1 \pm 1.4 \ \mu\text{b/GeV}$$

and

$$k_\Lambda = 2.03 \pm 0.01 \ \text{GeV}^{-1}$$

for $1.4 < M_X < 2.4$ GeV

(χ^2 probability = 87%).

The slope of $d\sigma/dM_X$ for inclusive $\overline{K}^0$ production is similar to that obtained for the reaction $K^+p \to K^0X^{++}$ at 5 GeV/c,[13] which was found to be 2.10 ± 0.05 GeV^{-1}.

The Lorentz-invariant differential cross section $f(x)$ is defined as

$$f(x) = \int \frac{E_V^*}{p_K^*} \frac{d^2\sigma}{dx\,dp_T^{\,2}}\, dp_T^{\,2},$$

with $x = p_L^*/p_K^*$. In this expression, p_{K^-} is the incident K^- momentum, E_V the total energy of the V^0, and p_L and p_T are longitudinal and transverse momenta of the V^0 with respect to the incident K^-; an asterisk denotes center-of-mass quantities. The Feynman-x distributions for reaction (1) as a function of topology are shown in Fig. 6. The distributions are typical of beam fragmentation; a clear suppression of backward $\overline{K}^0$ production is observed, in agreement with data at lower and higher energies.[3,6] In the absence of appreciable

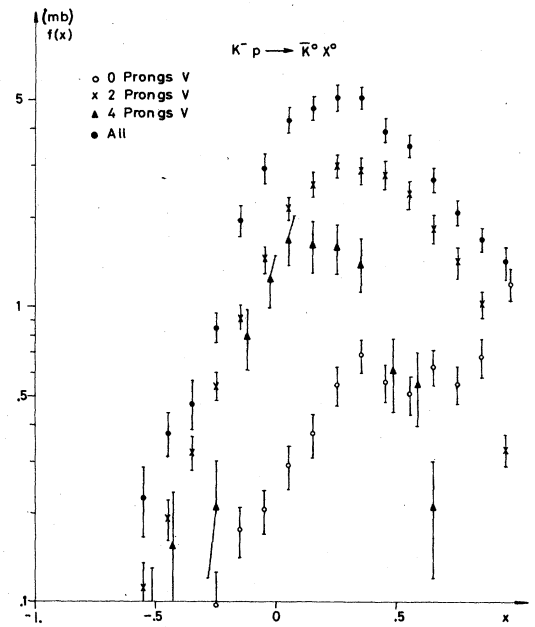

FIG. 6. The Lorentz-invariant differential cross section $f(x)$ for the reaction $K^-p \to \overline{K}^0 X$ for different topologies.

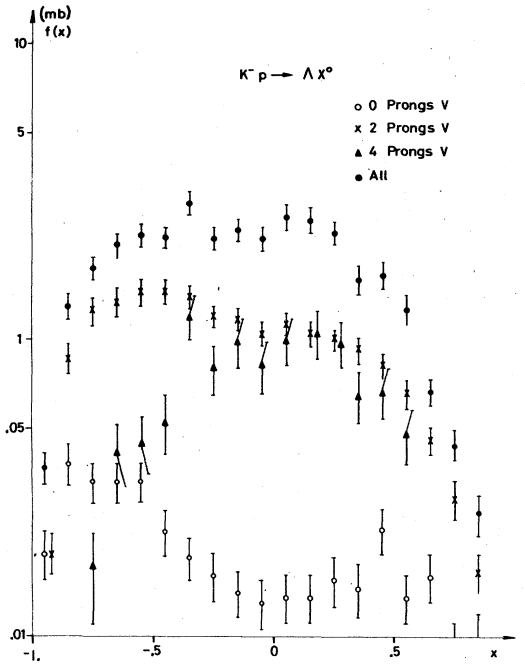

FIG. 7. The Lorentz-invariant differential cross section $f(x)$ for the reaction $K^-p \to \Lambda^0 X$ for different topologies.

multikaon production, backward $\bar{K}^0$ emission would correspond to exotic t-channel exchanges [see Fig. 1(b)], whereas forward $\bar{K}^0$ production is consistent with a leading-particle effect at the meson vertex. For the zero-prong V^0 topology the charge-exchange neutron (or N^*) production noted in Fig. 4 accounts for the rise in $f(x)$ near $x=1$. Also, it can be seen that $\bar{K}^0$ production becomes more central as the charged-prong multiplicity increases.

Figure 7 shows the $f(x)$ distribution for Λ^0 production via reaction (2). It indicates significant production of both forward (fast, beamlike) and backward (slow, targetlike) Λ^0 particles. The zero- and two-prong contributions show predominance of targetlike Λ^0 production, while for the four prongs $f(x)$ is more symmetric and more central. The asymmetries of the x distributions in the zero- and two-prong topologies suggest that their Λ^0 production mechanisms have a large contribution of strange meson exchange or proton fragmentation. It is also seen that the relative importance of baryon exchange, leading to beamlike Λ^0 production, increases with prong number. However, the increase in $\bar{K}^0$ and Λ^0 production in the central region with emitted number of charged particles may be partially of kinematic origin, as can be seen from the kinematic relation:

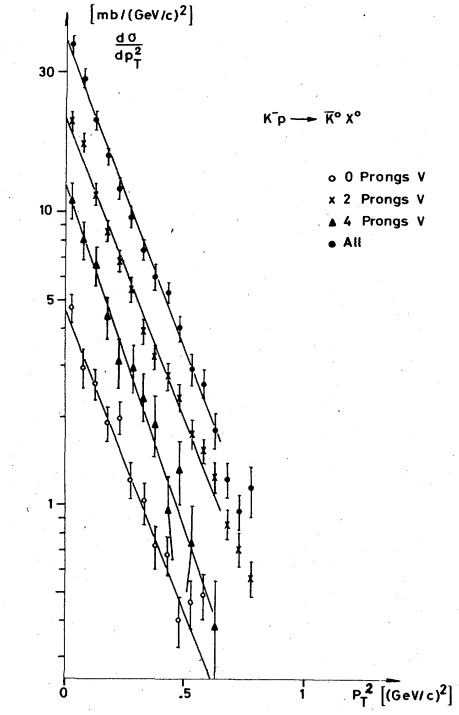

FIG. 8. Cross section as a function of the transverse momentum squared of the $\bar{K}^0$ produced in the reaction $K^-p \to \bar{K}^0 X$, displayed for each topology. The solid lines are the results of fits to the expression $d\sigma/dp_T^2 = Ae^{-Bp_T^2}$ (Table II).

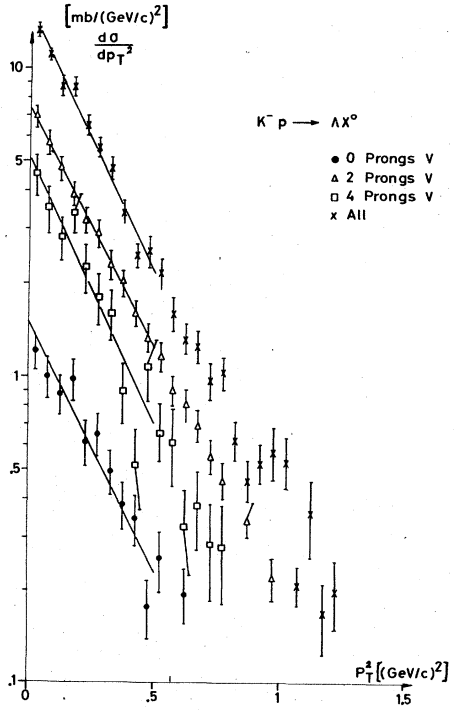

FIG. 9. Cross section as a function of the transverse momentum squared of the Λ^0 produced in the reaction $K^-p \to \Lambda^0 X$, displayed for each topology. The solid lines are fits to the expression $d\sigma/dp_T^2 = Ae^{-Bp_T^2}$ (Table II).

$$x^2 = \frac{(s + m_{V^0}{}^2 - M_X{}^2)^2}{s^2} - \frac{4M_{V^0}{}^2}{s} - \frac{4p_T{}^2}{s} .$$

Since the distributions of the missing mass squared $M_X{}^2$ are concentrated at higher values when the prong number increases (Figs. 4 and 5), high $|x|$ values should be correspondingly suppressed.[14]

The transverse-momentum dependence of the cross section $d\sigma/dp_T{}^2$ for $\overline{K}{}^0$ and Λ^0 production is displayed in Figs. 8 and 9. The slope for inclusive $\overline{K}{}^0$ production is steeper than that for Λ^0 production, in agreement with the increase of average transverse momentum with the mass of the secondary observed at other energies[7] and for other types of beam particles. Results of fits of the overall and topological distributions to an exponential form $d\sigma/dp_T{}^2 = Ae^{-Bp_T{}^2}$ are shown in Table II. No significant dependence on topology of the slopes of the distributions at low p_T [$P_T{}^2 < 0.7$ (GeV/c)^2] is observed.

The distribution of the four-momentum transfer $t' = |t - t_{\min}|_{K^- \to \overline{K}{}^0}$ for $\overline{K}{}^0$ production via reaction (1), displayed in Fig. 10, is approximately exponential with little structure, as was previously observed in K^-p experiments at 4.2 and 10.1 GeV/c. The t' distribution for Λ^0 production via reaction (2) is shown in Fig. 11, where t'

TABLE II. Fits to transverse momentum squared and four-momentum transfer squared distributions.

(a) $K^-p \to \overline{K}{}^0 X^0$

$d\sigma/dp_T{}^2 = Ae^{-Bp_T{}^2}$

n_c	$\lvert x\rvert_{\max}$	A [mb/(GeV/c)^2]	B [(GeV/c)$^{-2}$]	Range [(GeV/c)^2]	χ^2 prob. (%)
0	0.99	4.72 ± 0.19	4.81 ± 0.13	<0.065	29
2	0.97	21.26 ± 0.59	4.79 ± 0.08	<0.065	47
4	0.91	12.09 ± 1.19	5.37 ± 0.37	<0.065	97
All		38.87 ± 0.96	4.98 ± 0.08	<0.065	81

$d\sigma/dt' = A_1 e^{-B_1 t'}$

n_c	$\lvert x\rvert_{\max}$	A_1 [mb/(GeV/c)^2]	B_1 [(GeV/c)$^{-2}$]	Range [(GeV/c)^2]	χ^2 prob. (%)
0	0.99	1.17 ± 0.07	1.18 ± 0.06	≤2.0	85
2	0.97	5.09 ± 0.24	1.19 ± 0.04	≤2.0	71
4	0.91	1.66 ± 0.09	0.70 ± 0.10	≤2.0	10
All		8.11 ± 0.15	1.05 ± 0.02	≤2.0	37

(b) $K^-p \to \Lambda^0 X^0$

$d\sigma/dp_T{}^2 = Ae^{-Bp_T{}^2}$

n_c	$\lvert x\rvert_{\max}$	A [mb/(GeV/c)^2]	B [(GeV/c)$^{-2}$]	Range [(GeV/c)^2]	χ^2 prob. (%)
0	0.99	1.44 ± 0.13	3.68 ± 0.33	<0.50	33
2	0.98	7.45 ± 0.23	3.59 ± 0.11	<0.50	77
4	0.96	5.07 ± 0.31	3.96 ± 0.52	<0.40	53
All		15.00 ± 0.36	3.88 ± 0.18	<0.50	39

$d\sigma/dt' = A_1 e^{-B_1 t'}$

n_c	$\lvert x\rvert_{\max}$	A_1 [mb/(GeV/c)^2]	B_1 [(GeV/c)$^{-2}$]	Range [(GeV/c)^2]	χ^2 prob. (%)
0	0.99	0.398 ± 0.033	1.87 ± 0.19	≤1.0	98
2	0.98	2.11 ± 0.07	1.66 ± 0.06	≤1.0	86
4	0.96	0.833 ± 0.117	1.17 ± 0.28	≤1.0	53
All		3.37 ± 0.10	1.50 ± 0.06	≤1.0	65

$d\sigma/du' = A_2 e^{-B_2 u'}$

n_c	$\lvert x\rvert_{\max}$	A_2 [mb/(GeV/c)^2]	B_2 [(GeV/c)$^{-2}$]	Range [(GeV/c)^2]	χ^2 prob. (%)
0	0.99	0.12 ± 0.01	0.87 ± 0.07	≤2.0	25
2	0.98	0.69 ± 0.01	0.57 ± 0.02	≤2.0	84
4	0.96	0.46 ± 0.06	0.41 ± 0.11	≤2.0	22
All		1.38 ± 0.05	0.53 ± 0.03	≤2.0	24

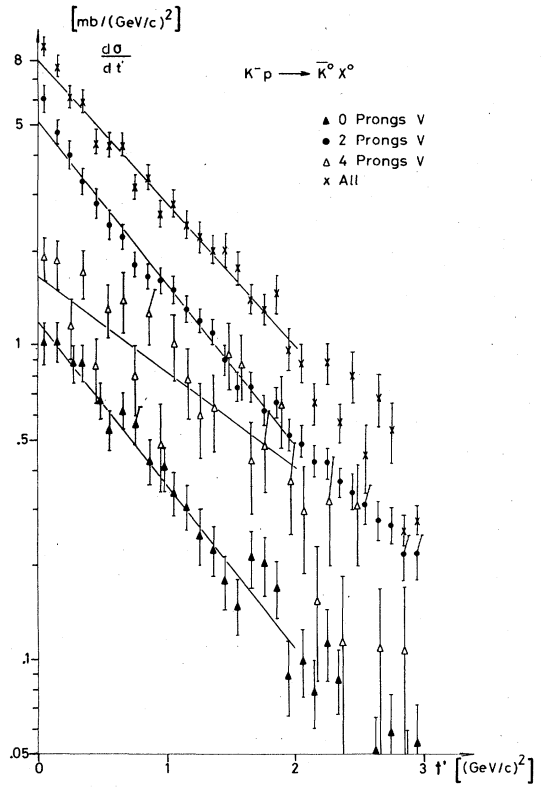

FIG. 10. The topological distributions of the four-momentum transfer $t' = |t - t_{\min}|_{K^- \to \bar{K}^0}$ for $\bar{K}^0$ production via the reaction $K^-p \to \bar{K}^0 X$. The solid lines are fits to exponential expressions (Table III).

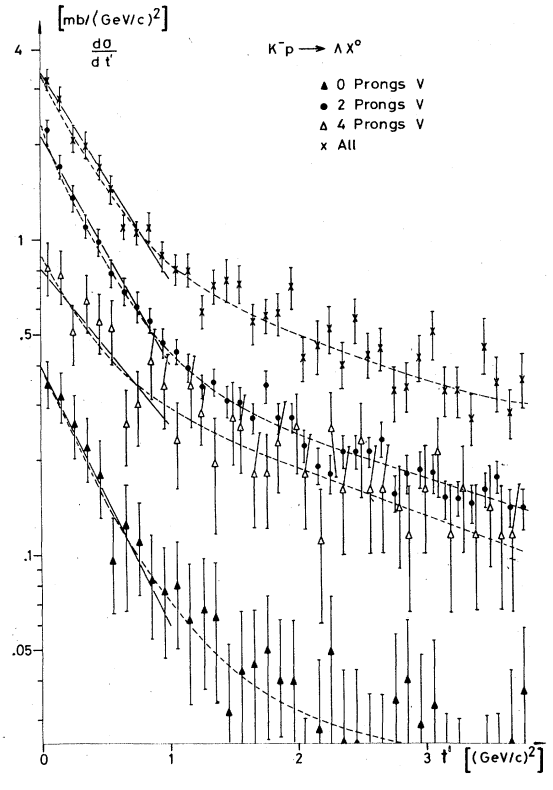

FIG. 11. The topological distributions of the four momentum transfer $t' = |t - t_{\min}|_{p \to \Lambda^0}$ for Λ^0 production via the reaction $K^-p \to \Lambda^0 X$. The solid lines are the results of fits to exponential expressions (Table III).

$= |t - t_{\min}|_{p \to \Lambda^0}$. The two-component slope seen in other experiments is also observed here. The steep slope of the t' dependence at four momentum transfers $t' < 1.0$ (GeV/c)^2 tends to decrease with increasing charge multiplicity.

In Figs. 12 and 13 the inclusive u' distributions are shown for $\bar{K}^0$ and Λ^0 production, respectively. We define u' such that

$$u' = |u - u_{\min}|_{p \to \bar{K}^0} \text{ and } u' = |u - u_{\min}|_{K^- \to \Lambda^0}.$$

The number of two-prong $\bar{K}^0$ events observed at small u' in Fig. 12 implies the presence of target fragmentation into $\bar{K}^0$ + hyperon or strange particle exchange processes. The zero-prong and four-prong $\bar{K}^0$ events exhibit forward dips in $d\sigma/du'$ and hence show no dominant contribution of u-channel exchange. The distribution at large u' is broad and decreases as one approaches the kinematic limit. The peaks in the u' distributions of Fig. 13, which correspond to forward Λ^0 production and which are most noticeable in the zero-prong events, reflect the presence of nucleon exchange. This same feature was noted in 10.1-GeV/c K^-p data (Bartsch *et al.*, Ref. 6).

The results of exponential fits ($d\sigma/dt' = A_1 e^{-B_1 t'}$) to the low-$t'$ peaks observed in both $\bar{K}^0$ and Λ^0 production, and to the peak at low u' values ($d\sigma/du' = A_2 e^{-B_2 u'}$) found in Λ^0 production, are displayed in Table II. In all cases, the slope parameters B_1 or B_2 decrease with increasing multiplicity.[15]

The single-component structure of the t' and u' distributions for $\bar{K}^0$ mesons as opposed to the two-component behavior observed in the corresponding Λ^0 distributions, reflect the dominance of beam fragmentation in $\bar{K}^0$ production versus the occurrence of abundant target (peak at small t') and beam fragmentation (peak at small u') in Λ^0 production. From a fit (Table III) of the t' and u' distributions for the Λ particles to the expressions

$$d\sigma/dt' = a_1 e^{-b_1 t'} + a_2 e^{-b_2 t'}$$

and

$$d\sigma/du' = \alpha_1 e^{-\beta_1 u'} + \alpha_2 e^{-\beta_2 u'},$$

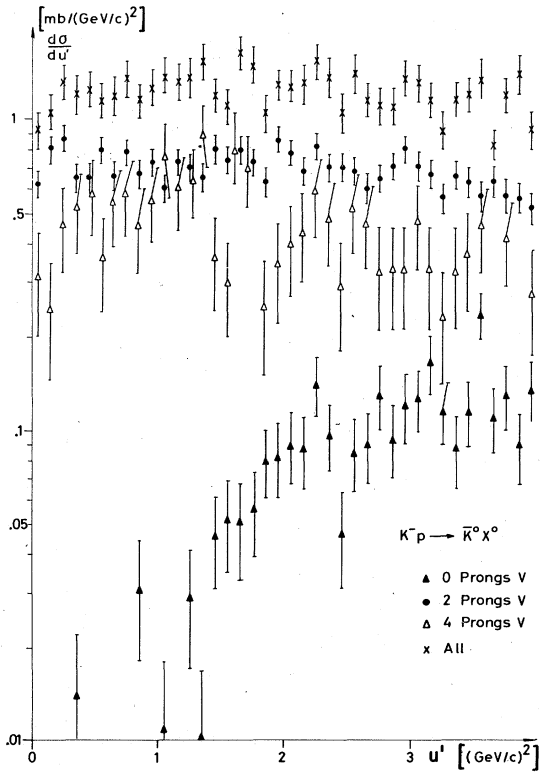

FIG. 12. The topological distributions of the four-momentum transfer $u' = |u - u_{\min}|_{p \to \bar{K}^0}$ for $\bar{K}^0$ production via the reaction $K^- p \to \bar{K}^0 X$. The solid lines are fits to exponential expressions (Table III).

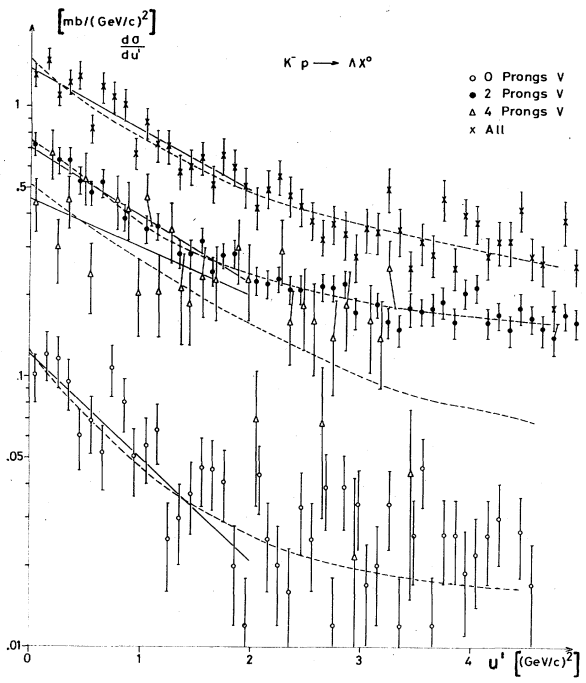

FIG. 13. The topological distributions of the four-momentum transfer $u' = |u - u_{\min}|_{K^- \to \Lambda^0}$ for Λ^0 production via the reaction $K^- p \to \Lambda^0 X$. The solid lines are fits to exponential expressions (Table III).

we find $\sigma_\Lambda(p) \sim 1$ mb and $\sigma_\Lambda(K^-) \sim 0.6$ mb, where $\sigma_\Lambda(p)$ and $\sigma_\Lambda(K)$ are estimates of Λ production in target- and beam-fragmentation regions, for which diagrams 1(c) and 1(d) should give dominant contributions. In the beam-fragmentation region (at low t'), it can be seen from Table III that the slope parameter has a tendency to increase with topology when a double exponential is fitted, contrary to the decrease obtained when using the simple exponential fit.

The Λ^0 events can be separated into two distinct "target-" and "beam-fragmentation" samples by imposing $t' < 1$ (GeV/c)^2 and $u' < 2$ (GeV/c)^2 cuts,

TABLE III. Fits of the t' and u' distributions of Λ^0 hyperons to the sum of two exponentials.

	$d\sigma/dt' = a_1 e^{-b_1 t'} + a_2 e^{-b_2 t'}$					
n_c	a_1 [mb/(GeV/c)^2]	b_1 [(GeV/c)$^{-2}$]	a_2 [mb/(GeV/c)^2]	b_2 [(GeV/c)$^{-2}$]	Range [(GeV/c)^2]	χ^2 Prob. (%)
0	0.37 ± 0.06	2.18 ± 0.37	0.04 ± 0.005	0.13 ± 0.07	$t' < 4.0$	99
2	1.93 ± 0.13	2.70 ± 0.20	0.43 ± 0.01	0.31 ± 0.02	$t' < 4.0$	99
4	0.56 ± 0.11	3.13 ± 0.84	0.38 ± 0.02	0.35 ± 0.03	$t' < 4.0$	98
All	2.80 ± 0.23	2.63 ± 0.16	0.87 ± 0.03	0.29 ± 0.03	$t' < 4.0$	99
	$d\sigma/du' = \alpha_1 e^{-\beta_1 u'} + \alpha_2 e^{-\beta_2 u'}$					
n_c	α_1 [mb/(GeV/c)^2]	β_1 [(GeV/c)$^{-2}$]	α_2 [mb/(GeV/c)^2]	β_2 [(GeV/c)^2]	Range [(GeV/c)^2]	χ^2 Prob. (%)
0	0.10 ± 0.01	1.37 ± 0.21	0.024 ± 0.006	0.09 ± 0.02	$u' \leq 5.0$	2
2	0.58 ± 0.02	1.05 ± 0.04	0.18 ± 0.004	0.025 ± 0.006	$u' \leq 5.0$	9
4	0.44 ± 0.04	0.83 ± 0.07	0.09 ± 0.01	0.10 ± 0.03	$u' \leq 5.0$	0
All	0.93 ± 0.06	1.16 ± 0.09	0.57 ± 0.02	0.17 ± 0.09	$u' \leq 5.0$	6

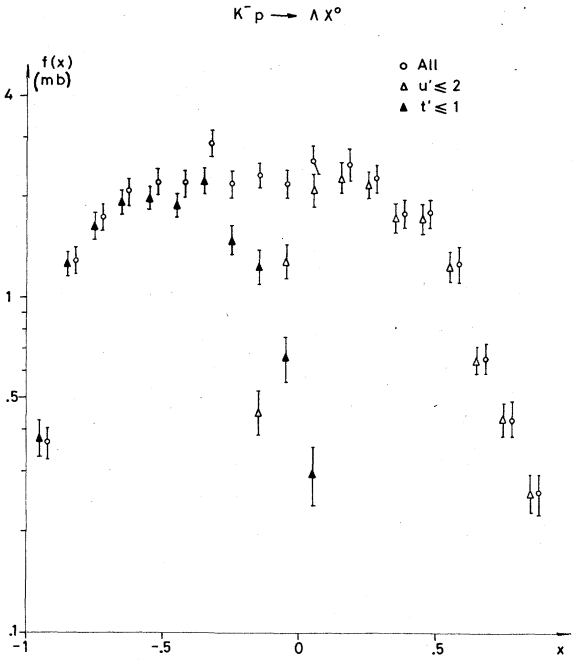

FIG. 14. The $f(x)$ distribution for inclusive Λ^0 production. Also shown are the corresponding $f(x)$ distributions for Λ^0 particles with the four-momentum-transfer selections $t' < 1$ (GeV/c)^2 and $u' < 2$ (GeV/c)^2 (see text).

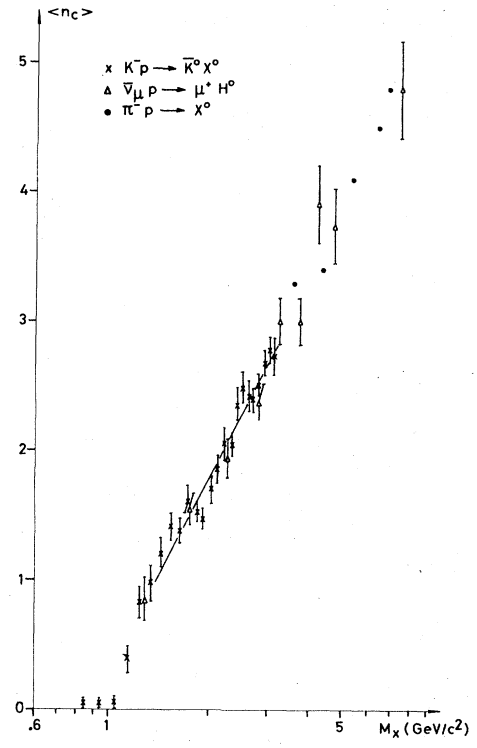

FIG. 15. The average charge multiplicity $\langle n_c \rangle$ as a function of the mass of the recoil hadronic system M_X for the reaction $K^-p \to \bar{K}^0 X$ in this experiment. Results are compared to charge multiplicities in the processes $\pi^-p \to X$ (inclusive) and $\nu p \to \mu^+ X^0$.

respectively, is shown in Fig. 14. By taking these cuts to define backward and forward production of inclusive Λ^0's, one obtains $\sigma_\Lambda(p) = 1.75 \pm 0.11$ mb and $\sigma_\Lambda(K^-) = 1.76 \pm 0.11$ mb. A rough measure of forward and backward inclusive $\bar{K}^0$ production can be defined in the same way [$t' < 1$ (GeV/c)^2 and $u' < 2$ (GeV/c)^2, respectively], yielding $\sigma_{\bar{K}^0}(p) = 5.08 \pm 0.32$ mb and $\sigma_{\bar{K}^0}(K^-) = 2.53 \pm 0.15$ mb.

V. UNIVERSAL FEATURES OF MULTIPARTICLE PRODUCTION

Charge-multiplicity distributions have been studied for K^0_S and Λ^0 events as a function of $\ln M_X$. As shown in Fig. 15, the dependence of the average charge multiplicity $\langle n_c \rangle$ of the hadronic system re-

TABLE IV. Dependence of the average charged multiplicity of a hadronic system X on the available rest energy M_X.

Reaction	Range of M_X [(GeV/c)^2]	$\langle n_c \rangle = a + b \ln M_X$ a	b	χ^2/NDF	$\langle n_c \rangle = a' + b' \ln M_X + c' \ln^2 M_X$ a'	b'	c'	χ^2/NDF
$K^-p \to \bar{K}^0 X$[a]	1.4 to 3.2	0.27 ± 0.02	2.17 ± 0.03	1.56	1.00 ± 0.29	0.09 ± 0.79	1.33 ± 0.03	1.2
$\pi^-p \to X$	4.4 to 20.0	−0.31 ± 0.03	2.70 ± 0.06	10.68	0.59 ± 0.10	1.62 ± 0.12	0.30 ± 0.03	2.83
$\bar{\nu}_\mu p \to \mu^+ X$	1.0 to 7.0	0.06 ± 0.06	2.44 ± 0.06	...	...	...	...	...
$K^-p \to \Lambda X$[a]	1.3 to 2.6	1.05 ± 0.11	2.22 ± 0.17	0.73	1.56 ± 0.33	0.28 ± 0.12	1.63 ± 0.97	0.51
$K^+p \to K^0 X$	1.6 to 3.6	0.98 ± 0.04	1.84 ± 0.04	7.11	...	...	...	...
$K^-p \to \Lambda(p) X$[a]	1.3 to 2.6	1.07 ± 0.04	2.18 ± 0.06	0.69	1.25 ± 0.04	1.47 ± 0.16	0.60 ± 0.08	0.72
$K^-p \to \Lambda(K) X$[a]	1.3 to 2.6	0.66 ± 0.05	2.98 ± 0.08	0.56	0.74 ± 0.11	2.68 ± 0.07	0.23 ± 0.09	0.63
$\bar{p}p \to$ mesons	1.85 to 3.9	1.69 ± 0.36	2.15 ± 0.36	0.60	...	...	...	...

[a] This experiment. $\Lambda(p)$ and $\Lambda(K)$ refer to proton and kaon fragmentation respectively.

coiling against the neutral kaon is roughly linear. The inclusive cross sections for single- and double-V^0 production at 6.5 GeV/c (Sec. III) suggest that ~80% of events containing an associated K_S^0 originate from $\bar{K}^0$ rather than K^0 production. *Assuming* that K_S^0 events predominantly reflect $\bar{K}^0$ (K^0) production characteristics in K^-p (K^+p) interactions, it is of interest to compare the dependence of $\langle n_c \rangle$ upon $\ln M_X$ for $K^-p \to \bar{K}^0 X$ to processes $\pi^-p \to X$[16] and $\bar{\nu}_\mu p \to \mu^+ X$,[17] since the hadronic systems X have the same additive quantum numbers. That the same dependence characterizes all of these hadronic systems is evident from Fig. 15 and also from Table IV, which summarizes fits of all these data to the form $\langle n_c \rangle = a + b \ln M_X$. A linear slope parameter $b \simeq 2$ is common to hadronic systems in the invariant-mass range probed in this experiment. However, quantum-number conservation can strongly influence the value of the parameter a. This is illustrated for charge and baryon number by Fig. 16; the data for $K^-p \to \bar{K}^0 X^0$ ($B=1$) are compared to the inclusive Λ^0 data from the present experiment $K^-p \to \Lambda^0 X^0$ ($B=0$) and to results from a study of the process $K^+p \to K^0 X^{++}$ ($B=1$). Although a linear fit to the latter data is poor (see Table IV), the average multiplicity at a given M_X value is found to be higher in K^+ than in K^- induced reactions leading to K_S^0 production, as expected. Above the resonance region ($M_X > 1.5$ GeV), dependence of $\langle n_c \rangle$ on $\ln M_X$ is found to be linear for both $\bar{K}^0$ and Λ^0 production. The slope parameters are equal within errors, and the systematic shift in M_X at fixed $\langle n_c \rangle$ is of the order of the nucleon-pion mass difference.

It is of interest to subdivide the Λ^0 events into target-$[t' < 1\ (\mathrm{GeV}/c)^2]$ and beam-fragmentation samples $[u' < 2\ (\mathrm{GeV}/c)^2]$ in order to isolate virtual $K\bar{K}$ and $B\bar{B}$ annihilation processes, respectively. Distributions of $\langle n_c \rangle$ versus M_X are shown in Fig. 17 for these restricted samples from which events containing two visible V^0's were removed in order to reduce background from nonannihilation reactions. No appreciable difference between the annihilation-enriched samples is found, in agreement with comparison undertaken in 4.2-GeV/c K^-p data.[3] As also noted in other data,[16] the variation of $\langle n_c \rangle$ with M_X recoiling from produced Λ^0's extrapolates smoothly onto $\bar{p}p \to n\pi$ annihilation data for $M_X = \sqrt{s} > 2$ GeV, where $\sqrt{s}$ is the center-of-mass energy available in the $\bar{p}p$ reaction.

The M_X dependence of charge-multiplicity moments of the residual system, as indicated by

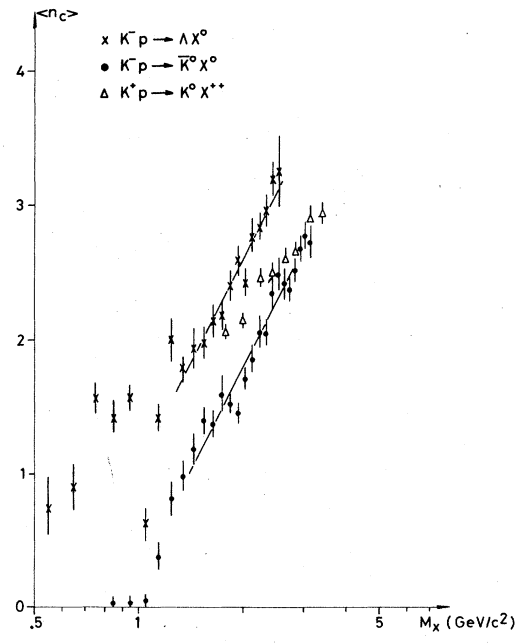

FIG. 16. The average charge multiplicity $\langle n_c \rangle$ of the neutral hadronic system X^0 versus invariant mass M_X, for the processes $K^-p \to \bar{K}^0 X$, $K^+p \to K^0 X^{++}$, and $K^-p \to \Lambda^0 X^0$.

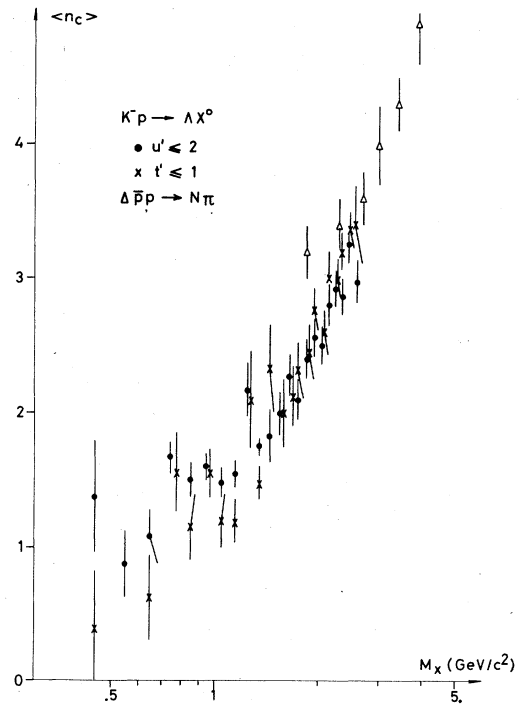

FIG. 17. The average charge multiplicity $\langle n_c \rangle$ of the hadronic system X^0 versus invariant mass M_X for the reaction $K^-p \to \Lambda^0 X^0$ containing only one visible V^0 for both $t' < 1\ (\mathrm{GeV}/c)^2$ and $u' < 2\ (\mathrm{GeV}/c)^2$. Also displayed are corresponding results for the annihilation reaction $\bar{p}p \to X^0$ (mesons).

$\langle n_c \rangle / D$ and by the correlation coefficient f_2^{cc}, is given in Figs. 18 and 19. The ρ^0 region is seen to be slightly enhanced in the $\langle n_c \rangle / D$ distribution of Fig. 18(a), as expected if the dispersion $D = (\langle n_c^2 \rangle - \langle n_c \rangle^2)^{1/2}$ is reduced by the contribution of $\rho^0 \to \pi^+ \pi^-$ decay. All distributions from this experiment are found to join smoothly from low M_X values onto distributions obtained from systems having identical additive quantum numbers. These results are in accordance with the universal behavior of multiparticle production expected from quark interaction models.[9]

The success of quark-parton models in describing regularities of lepton-induced reactions has led to attempts to explain the fundamentals of hadron-induced reactions by invoking similar mechanisms. In the framework of these models, the initial interaction between fragmenting hadrons can proceed by either of two distinct perturbation-theory mechanisms: (i) exchange of vector gluons, of (ii) "wee"-quark exchange or annihilation. As noted by Brodsky and Gunion, the universality in inelastic multiplicities observed in lepton- and hadron-induced reactions is evidence for the dominance of the quark-exchange/annihilation contribution over that of gluon exchange. In the work of Brodsky and Gunion,[10] single- and double-fragmentation cross sections at Fermilab and CERN ISR energies are shown to agree with power-law behavior expected from the quark-exchange/annihilation mechanism. However, the formalism is not specifically restricted to fragmentation reactions at high incident mo-

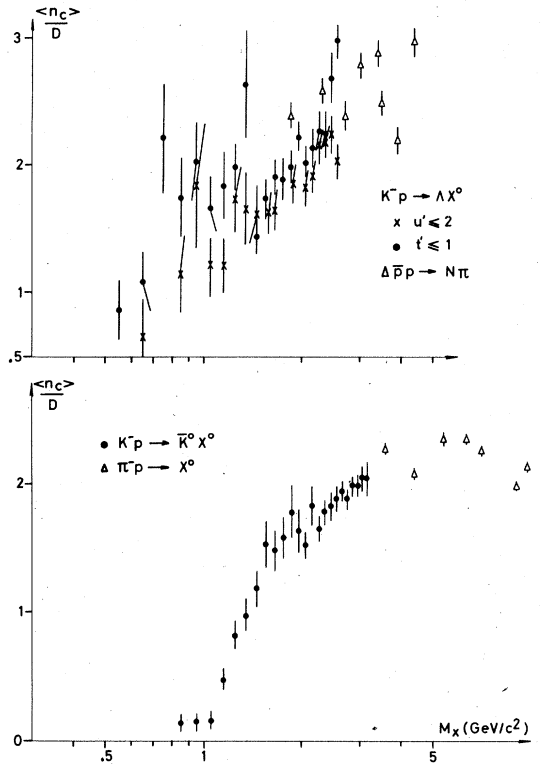

FIG. 18. Comparison of the mass dependence of the ratio $\langle n_c \rangle / D$ for various hadronic systems having identical additive quantum numbers.

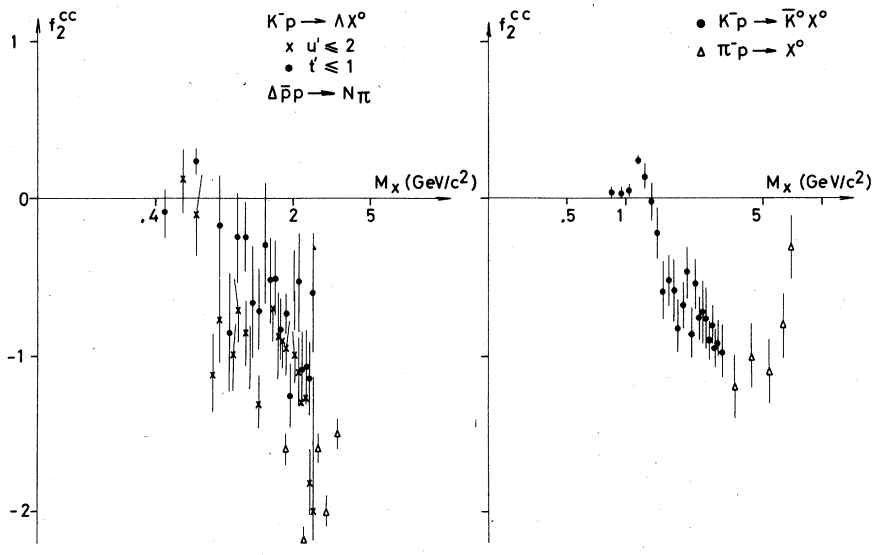

FIG. 19. Comparison of the mass dependence of the correlation coefficient f_2^{cc} between charged particles for various hadronic systems having identical additive quantum numbers.

mentum, and it is of interest to test the quark-exchange/annihilation predictions at 6.5 GeV/c, where universal behavior of hadronic systems is also prominent. Brodsky and Gunion give definite predictions for inclusive Λ^0 production in the fragmentation regions, namely

$$d\sigma/dX_\Lambda \propto (1-X_\Lambda) \quad \text{for } p \to \Lambda, \tag{5}$$

$$\propto (1-X_\Lambda)^3 \quad \text{for } K^- \to \Lambda, \tag{6}$$

if the Λ^0 production is initiated by single "wee" quark annihilation/exchange, whereas

$$d\sigma/dX_\Lambda \propto (1-X_\Lambda)^3 \quad \text{for } p \to \Lambda, \tag{7}$$

$$\propto (1-X_\Lambda)^5 \quad \text{for } K^- \to \Lambda, \tag{8}$$

if gluon exchange or dissociation dominates. In these expressions the overall normalizations are arbitrary, and $X_\Lambda = E^*_\Lambda / E^{*\max}_\Lambda$ is the radial scaling variable. In the absence of an event-by-event jet-direction analysis, X_Λ should be the best approximation to the light-cone fraction at lower energies.[10]

The distribution $d\sigma/dX_\Lambda$ for the range $0.6 < X_\Lambda < 1$ in $K^- \to \Lambda^0$ fragmentation is shown in Fig. 20(a), for events which satisfy the selection $u' < 2$ (GeV/c)^2. The solid curve superimposed on the data represents a fit to the form $d\sigma/dX_\Lambda = C_1(1 - X_\Lambda)^3 + C_2$, for which $C_1 = 117.6 \pm 7.8$ mb, $C_2 = 0.134 \pm 0.015$ mb, with $\chi^2/\text{NDF} = 5.2/6$. In Fig. 20(b), it is shown that the slope of the $f(X_\Lambda)$ distribution for the process $p \to \Lambda^0$ [$t' < 1$ (GeV/c)^2] in the range $0.6 < X_\Lambda < 1.0$ also follows a simple power law. A fit to the expression $d\sigma/dX_\Lambda = C_1(1 - X_\Lambda) + C_2$ yields $C_1 = 7.9 \pm 0.6$ mb, $C_2 = 0.09 \pm 0.05$ mb, with $\chi^2/\text{NDF} = 8.8/4$. Similar fits to the predictions (7) and (8) for gluon exchange yield $\chi^2/\text{NDF} = 40.0/6$ for $K^- \to \Lambda^0$ fragmentation and $\chi^2/\text{NDF} = 30.8/4$ for $p \to \Lambda^0$ fragmentation. It is evident that our data are in agreement with dominance of the initial Λ^0 production process by single-quark exchange in both beam- and target-fragmentation regions. It should be noted that the expressions fitted correspond to minimal powers of $(1 - X_\Lambda)^n$ derived from quark counting; a mixture of powers could originate from exchanges of additional $q\bar{q}$ pairs.

An asymptotic triple-Regge expression for the beam-fragmentation region ($K^- \to \Lambda^0$) can be written as

$$\frac{d\sigma}{d^3p_\Lambda/E_\Lambda} \propto (1 - |x|)^{1-2\alpha_{K\bar{\Lambda}}(t_{K\Lambda})},$$

where $\alpha_{K\bar{\Lambda}}$ is the leading Regge trajectory and x is Feynman x for the Λ^0. If one assumes a leading baryon Regge trajectory which is linearly rising, one expects a $(1 - |x|)^{7/4}$ power behavior. A fit of the Feynman-x distribution to this form for $K^- \to \Lambda^0$ fragmentation events yielded $\chi^2/\text{NDF} = 5.1/3$. Similarly, for the $p \to \Lambda^0$ fragmentation data, a power law $\propto (1 - |x|)^{0.6}$ is expected from

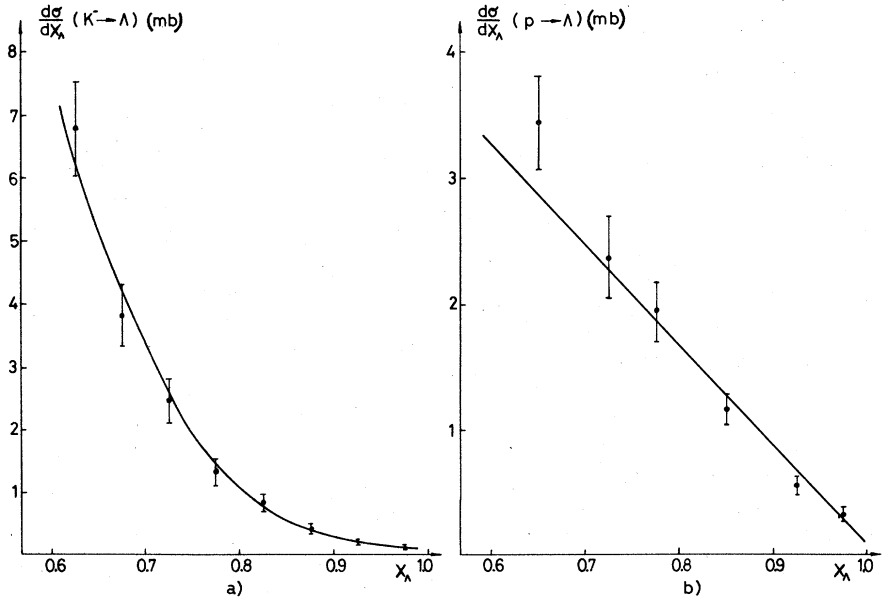

FIG. 20. The distribution in X_Λ, the radial scaling variable, for Λ^0 production by (a) beam fragmentation $K^- \to \Lambda^0$ [$u' < 2$ (GeV/c)^2], and (b) target fragmentation $p \to \Lambda^0$ [$t' < 1$ (GeV/c)^2]. The solid lines correspond to predictions of a quark-exchange/annihilation model (see text).

the triple-Regge formula assuming a leading K^* contribution. A fit to the data yielded a $\chi^2/\mathrm{NDF} = 8.0/3$. In both cases the goodness of fit can be improved by using additional Regge trajectory contributions in the asymptotic expression given above. We conclude that fragmentation distributions for $K^-p \to \Lambda^0 + X$ at 6.5 GeV/c can be accomodated in either the quark exchange of triple-Regge pictures.

VI. CONCLUSIONS

In K^-p interactions at 6.5 GeV/c:

(i) Inclusive $\bar{K}^0$ production proceeds predominantly via beam fragmentation; this effect is observed in both lower- and higher-energy K^-p reactions, and in K^0 production in K^+p reactions, throughout the intermediate energy range.

(ii) Inclusive Λ^0 differential cross sections show significant production of both beamlike and targetlike Λ^0's. The slope of the low t' and u' peaks and the relative contribution of beamlike processes decrease with increasing multiplicity.

(iii) The $Q = S = 0$ hadronic systems recoiling from V^0 particles have $B = 0$ and 1, respectively, for Λ^0 and $\bar{K}^0$ production. The dependence of $\langle n_c \rangle$, $\langle n_c \rangle / D$, and f_2^{cc} of these systems upon their invariant mass has been compared with the dependences exhibited by hadronic systems having identical quantum numbers, but produced in different processes. These comparisons indicate that universal aspects of multiparticle production, which were first delineated in high-incident-momentum collisions and which provided motivation for quark-interaction models, are prominent in $K^-p \to V^0 + X$ reactions at 6.5 GeV/c. For inclusive Λ^0 production at 6.5 GeV/c, both the $K^- \to \Lambda^0$ and the $p \to \Lambda^0$ fragmentation regions exhibit radial-scaling distributions predicted from an underlying quark-exchange/annihilation process.

ACKNOWLEDGMENTS

We wish to express our gratitude to the operating crews of the Argonne National Laboratory Zero Gradient Synchrotron, the 12-ft bubble chamber, and the rf-separated beam. We thank the scanning, measuring, and computing personnel at each of our respective laboratories. This research was supported by the IIKW and IISN, Belgium; by the U.S. Department of Energy; and by the National Science Foundation.

---

*Present address: Oxford University, Oxford, England.

[1] 3.0 GeV/c: D. Merrill *et al.*, Nucl. Phys. B18, 403 (1970).

[2] 3.93 and 14.3 GeV/c: A. Borg *et al.*, Nuovo Cimento 22A, 559 (1974).

[3] 4.2 GeV/c: R. Blokzijl *et al.*, Nucl. Phys. B39, 141 (1972); R. Blokzijl *et al.*, *ibid.* B98, 401 (1975); M. J. Losty *et al.*, *ibid.* B133, 38 (1978).

[4] 7.3 GeV/c: S. U. Chung *et al.*, Phys. Rev. D 11, 1010 (1975).

[5] 8.25 GeV/c: A. Vayaki *et al.*, Nucl. Phys. B58, 178 (1973); J. R. Fry *et al.*, *ibid.* B58, 408 (1973); E. Simopoulou *et al.*, *ibid.* B96, 413 (1975).

[6] 10.1 GeV/c: M. Aderholz *et al.*, Nucl. Phys. B5, 606 (1968); J. V. Beaupre *et al.*, *ibid.* B30, 381 (1971); J. Bartsch *et al.*, *ibid.* B40, 103 (1972).

[7] 10.1 and 16 GeV/c: P. Bosetti *et al.*, Nucl. Phys. B60, 307 (1973).

[8] 13.0 GeV/c: W. Barletta *et al.*, Phys. Rev. D 7, 3233 (1973); W. Barletta *et al.*, Nucl. Phys. B51, 499 (1973).

[9] See, for example, J. D. Bjorken and J. Kogut, Phys. Rev. D 8, 1341 (1973); S. J. Brodsky and J. F. Gunion, Phys. Rev. Lett. 37, 402 (1976), and in *Proceedings of the VII International Colloquium on Multiparticle Reactions, Tutzing, 1976*, edited by J. Benecke, J. Kuhn, L. Stodolsky, and F. Wagner (Max-Planck-Institut für Physik und Astrophysik, Munich, 1977); J. Dias de Deus and S. Jadach, Phys. Lett. 70B, 73 (1977); H. Satz, Nuovo Cimento 37A, 141 (1977).

[10] S. J. Brodsky and J. F. Gunion, Phys. Rev. D 17, 848 (1978).

[11] T. P. Wangler *et al.*, ANL Report No. ANL/HEP/7018, 1970 (unpublished).

[12] A notational convention which is common practice in the literature is used throughout this report: The symbol "$\bar{K}^0$" refers to measurement of $\bar{K}^0/K^0$ production in K^-p reactions and "K^0" refers to measurements of $K^0/\bar{K}^0$ in K^+p interactions. In Sec. V, dominance of negative- (positive-) strangeness neutral kaons from K^-p (K^+p) collisions is assumed in the analysis, and this assumption is explicitly stated in the text.

[13] P. V. Chliapnikov *et al.*, Phys. Lett. 52B, 375 (1974).

[14] The definition of $x = p_L^*/p_K^*$ used in this analysis yields effective values of $|x_{\max}|$ which are less than unity and which decrease slightly with increasing topology (see Table II).

[15] The observed systematic decrease of the slope of semi-inclusive $d\sigma/dt'$ and $d\sigma/du'$ distributions with charge multiplicity at low four-momentum transfer squared does not imply a similar systematic behavior of $d\sigma/dp_T^2$. Indeed, in the beam- (target-) fragmentation region $p_T^2 \simeq \langle |x| \rangle t'$ ($\simeq \langle |x| \rangle u'$) with an average value of $|x|$ which decreases with increasing multiplicity.

[16] J. Whitmore, Phys. Rep. 27C, 187 (1976).

[17] M. Derrick *et al.*, Phys. Rev. D 17, 1 (1978).